

07.2;13.3

## Low frequency noise and resistance in non-passivated InAsSbP/InAs based photodiodes in the presence of atmosphere with ethanol vapor

© M.E. Levinshtein<sup>1</sup>, B.A. Matveev<sup>1</sup>, N. Dyakonova<sup>2</sup>

<sup>1</sup>Ioffe Institute, St. Petersburg, Russia

<sup>2</sup>Laboratoire Charles Coulomb (L2C), University of Montpellier, CNRS, Montpellier, France

E-mail: melev@nimis.ioffe.ru

Received February 8, 2023

Revised April 6, 2023

Accepted April 11, 2023

Low frequency noise and electrical characteristics of the *p*-InAsSbP/*n*-InAs single photodiode heterostructures grown onto *n*<sup>+</sup>-InAs substrates have been measured in the presence of atmosphere containing ethanol vapor. Correlation between ethanol vapor density and electrical noise spectral density, as well as the heterostructure resistance, has been estimated, and possible reasons for such correlation have been discussed.

**Keywords:** InAs-photodiodes, hydrocarbon sensor, low-frequency noise, InAs natural surface oxide, surface-sensitive structures.

DOI: 10.61011/TPL.2023.06.56371.19524

The ability of oxide surface to change electrical resistance with varying composition of surrounding gas is widely utilized in developing various-purpose gas detectors. In fabricating such detectors, various materials are used, such as oxides of both *n*-type oxides (SnO<sub>2</sub>, ZnO, TiO<sub>2</sub>,  $\alpha$ -Fe<sub>2</sub>O<sub>3</sub>, WO<sub>3</sub>) and *p*-type oxides (CuO, NiO, Cr<sub>2</sub>O<sub>3</sub>, Co<sub>3</sub>O<sub>4</sub>), as well as In<sub>2</sub>O<sub>3</sub>–Ga<sub>2</sub>O<sub>3</sub> solid solution films. Detectors based on oxides and their solid solutions are sensitive to many various gases (analytes), for instance, to H<sub>2</sub>, NH<sub>3</sub>, CO, NO<sub>2</sub> and CH<sub>4</sub>; however, to ensure low gas-detection thresholds, high temperatures (up to 500°C) and high operating voltages (up to 2 V) are required [1–3]. This causes significantly increasing complexity of the detector structure due to both creation of an additional heating element [4] and necessity of providing conditions for efficient heat removal, which is hardly consistent with the problem of obtaining miniature devices.

Operating temperatures of surface-active sensors may be decreased with the aid of a natural oxide emerging on surfaces of most of studied semiconductors; thicknesses of such oxides vary from a few nanometers to a few micrometers. In InAs, the presence of an oxide film is followed by the Fermi level pinning and energy band bending on the surface with formation of a narrow conduction channel for electrons, which bypasses the semiconductor bulk conductivity [5]. When dry synthesized air is replaced with a mixture containing foreign impurities, room-temperature resistance of the oxide film on the InAs nanowire surface increases, which may be a base for sensors for water vapor/air humidity, ethanol, and other gases [6]. Notice that, according to the data given in [5], the oxide layer formed on the InAs surface etched with any etchant becomes 3–6 nm thick in as little as several minutes of exposure to air. Such a layer is non-stoichiometric, consists of a mixture of indium and arsenic oxides, contains also elemental arsenic

and other impurities, and is a source of field instability of MDS-structure electrophysical parameters (MDS means metal–dielectric–semiconductor).

In InAs photodiodes (PDs) or semiconductors with almost similar compositions, the presence of such an „electron“ channel leads to a decrease in the PD resistance and reduction of their detectability ( $D^*$ ). Therefore, development of methods for passivating surfaces and protective coatings for InAs-based PDs and semiconductors /semiconductor heterostructures with almost similar compositions still remains important [5,7]. An alternative (but not excluding the above ones) method for preventing surface currents (leakage currents) in photosensitive structures with InAs active regions consists in creating heterostructures containing additional „barrier“ layers with band gaps wider than that of InAs, for instance, AlAsSb [8] or InAsSbP layers [9–13].

On the other hand, variation in conductivity of the InAs PD electron channel in the atmosphere containing impurities may be used also for detecting those impurities themselves by measuring the resistance variation caused by the influence of the impurity contacting the surface. It is commonly believed that the PD surface conductivity is one of the main sources of its noise [7]. Thus, investigation of PD noise characteristics may be an additional source of information on a considered sample of air medium contacting the PD. A similar analysis of noises was performed for sensors based on various materials [3]; however, we have not found publications devoted to studying the influence of gas components on noise and resistance in InAs-based diodes.

In this work, we studied epitaxial structures isoperiodic with InAs, which were similar to those we have described earlier [10]; these epitaxial structures consisted of a highly doped *n*<sup>+</sup>-InAs substrate ( $n^+ \sim 10^{18} \text{ cm}^{-3}$ ), deliberately undoped active *n*-InAs layer 4–6  $\mu\text{m}$  thick, and wide-band-

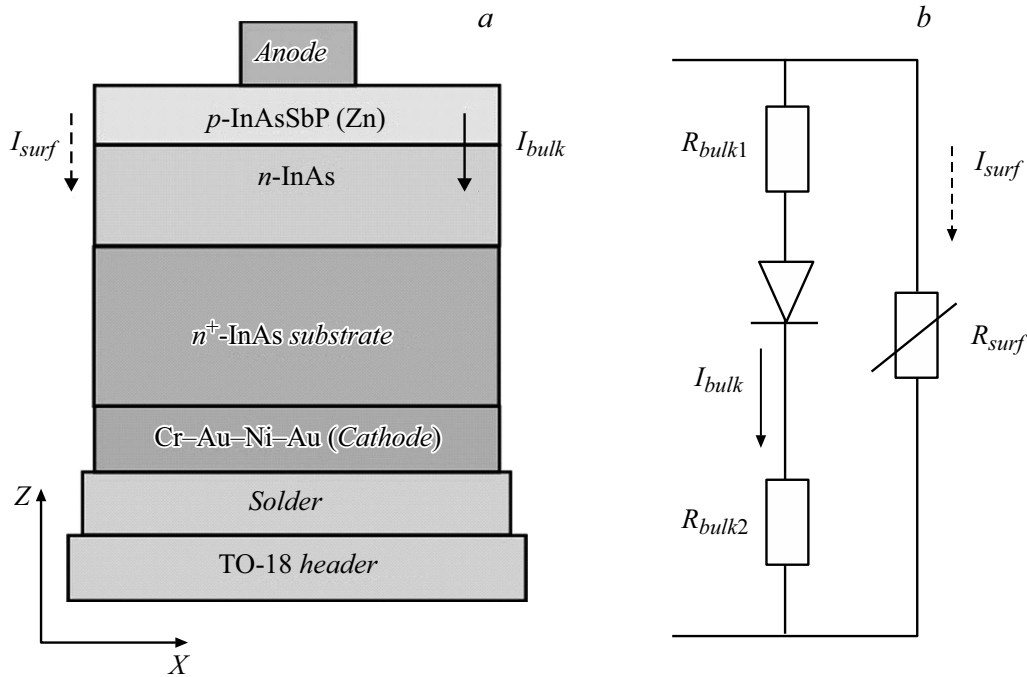


**Figure 1.** Schematic cross-section of the sample based on  $p$ -InAsSbP/ $n$ -InAs (a) and its simplified equivalent circuit (b). Axis  $Z$  — the direction of the epitaxial layer growth,  $R_{bulk1}$  — the contact resistance from the side of the anode and bulk resistance of the  $p$ -InAsSbP layer,  $R_{bulk2}$  — the contact resistance from the side of the cathode and bulk resistance of layers with the  $n$ -type conductivity,  $R_{surf}$ ,  $I_{surf}$  — the surface resistance and current over the structure surface,  $I_{bulk}$  — the bulk current.

gap layer of solid solution  $p$ -InAsSbP<sub>0.18</sub> 2–3  $\mu\text{m}$  thick doped with Zn during growing (Fig. 1, a). The band discontinuities at the heterointerface were  $\Delta E_c = 119$  meV and  $\Delta E_v = -30$  meV (300 K). In the case of lighting from the side of  $p$ -InAsSbP (3  $\mu\text{m}$  at 77 K and 3.4  $\mu\text{m}$  at 300 K), sensitivity in the spectral curve maximum was  $\sim 1$  A/W.

The PD chips had a square mesa  $330 \times 330 \mu\text{m}$  in area fabricated using conventional photolithography and „wet“ chemical etching. A disk metallic contact to the  $p$ -InAsSbP layer (anode)  $D_a = 80 \mu\text{m}$  in diameter was made by vacuum-thermal evaporation of metals and placed in the middle of the mesa. The contact to the substrate (cathode) was flush and occupied the entire area of the chip rear side. The samples were mounted with the substrate to TO-18 header as shown in Fig. 1, a; no measures were taken to prevent the chip lateral surfaces against contacting the air environment.

Fig. 1, b presents a schematic equivalent circuit of the sample where the total current has two components: the bulk one flowing through in-series connected resistances  $R_{bulk1}$ ,  $R_{bulk2}$  and  $p$ - $n$ -junction (current  $I_{bulk}$ ), and the surface one flowing through resistance  $R_{surf}$  (current  $I_{surf}$ ). As shown below, surface current  $I_{surf}$  changes its value under the impact of environment.

Low-frequency noise was studied in the frequency range of 1– $10^4$  Hz. The noise spectral density was measured in a circuit consisting of a photodiode, low-noise load resistance  $R_L$ , and power supply, all being connected in series. Current

fluctuations  $\delta I$  induced by the forward-biased PD were transformed at the load resistance to voltage fluctuations  $\delta U = \delta I R_L$  and fed first to preamplifier 5113 EG&G and then to spectrum analyzer Photon<sup>+</sup>. After subtracting the background noise, the current noise spectral density  $S_I$  was defined as  $S_I = S_U [(R_L + R_0)/(R_L R_0)]^2$ , where  $S_U$  is the spectral density of the voltage noise measured at the load resistance,  $R_0$  is the zero-bias photodiode resistance. The forward bias fed to PD was sufficiently low, due to which the diode differential resistance always remained equal to  $R_0$  (see the inset of Fig. 2).

The PD electrical characteristics were measured at room temperature (RT). PD was mounted above an open cuvette („bath“)  $30 \times 40$  mm in size filled with dehydrated ethanol. Distance  $h$  between the liquid surface and PD/  $p$ -InAsSbP surface was varied from 20 to 1 mm. The PD characteristics were also measured out of ethanol vapors and after submerging into liquid ethanol.

Fig. 2 presents the zero-bias resistance  $R_0$  versus measurement time  $t$  for PD both submerged in ethanol ( $60 < t < 100$  min) and withdrawn from it, i.e. in air ( $t > 100$  min).

As Fig. 2 shows, the presence of ethanol on the sample surface caused a significant decrease in the PD resistance due to an enhancement of the surface leakage currents in the presence of the analyte; these currents are designated in Fig. 1 as  $I_{surf}$ . Evidently, there are no apparent reasons

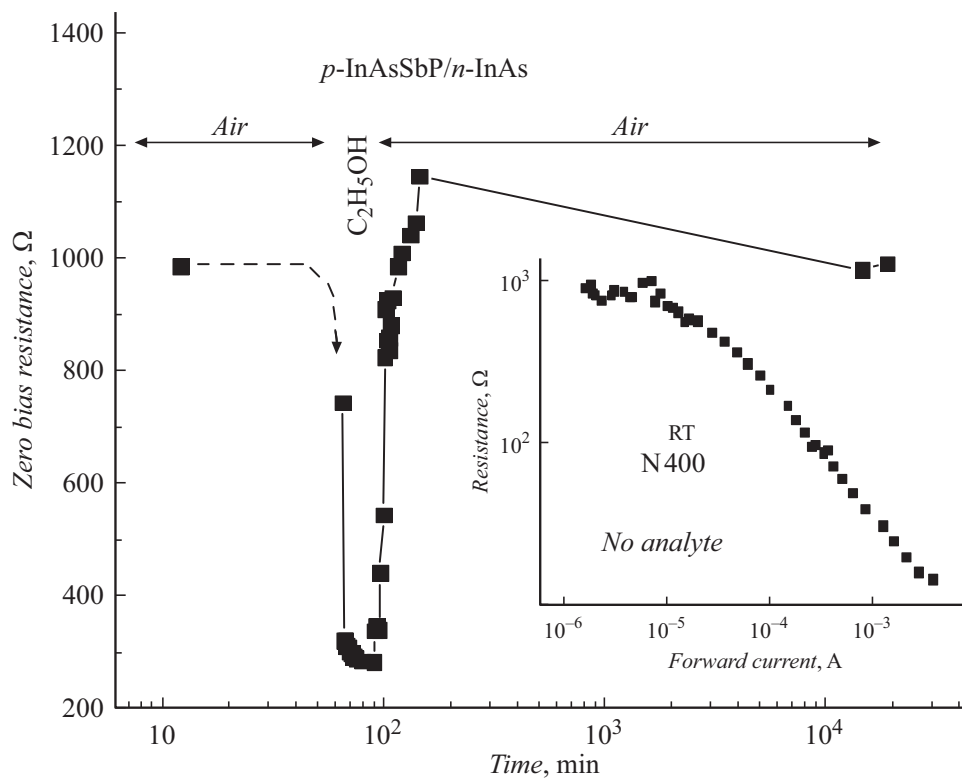


**Figure 2.** Zero-bias resistance  $R_0$  versus time  $t$  for the PD submerged in ethanol and after terminating the PD–ethanol contact. The inset presents the dependence of the initial differential resistance of the diode on forward current [10]. This dependence is highly-accurately reproducible due to sufficiently long exposure to air after withdrawing the structure from ethanol.

for variations in the resistance bulk components  $R_{bulk1}$  and  $R_{bulk2}$ .

After withdrawing the sample from ethanol, the stage of relatively fast variation in  $R_0$  ( $100 < t \leq 110$  min) took place, which was, evidently, associated with ethanol evaporation from the surface. This was followed by the stage of a relatively slow ( $110 \leq t \leq 200$  min) increase in the resistance, after which the resistance continued decreasing very slowly and returned to initial value  $R_0$ . Evidently, these slow processes were caused by restructuring of the spectrum of surface states occurring due to the PD contact with ethanol.

The PD characteristics changed also under the action of ethanol vapor upon the PD surface. Fig. 3 demonstrates the dependences of noise characteristics and resistance  $R_0$  on distance  $h$  between PD and liquid surface. The measurements were performed for each  $h$  in  $\sim 15$  min, when  $R_0$  stopped depending on time.

As shown by measurements similar to those described in [14,15] which were performed using diodes with immersion lenses mounted at distance  $L = 45$  mm from each other and not equipped with narrow-band filters, optical transmission  $T$  of the path arranged in parallel with the ethanol surface varied in the wavelength range  $\lambda = 3.4 \mu\text{m}$  depending on the distance to the liquid surface as  $T \propto \exp(-\chi/h)$  ( $\chi = 0.25$  mm), which indicates a

significant variation in the number of ethanol molecules in air with varying  $h$ . According to the data from a domestic alcohol detector, the ethanol concentration at  $h = 20$  mm was 0.04 vol.%. Data on the same optron calibrated using dry nitrogen–ethanol mixtures obtained at the D.I. Mendeleev Institute for Metrology showed that variation in its photocurrent  $I_{ph}$  at distance  $h = 20$  mm from the cuvette is equivalent to the  $I_{ph}$  variation caused by the presence in the optical path of ethane 0.05 vol.% in concentration.

At distances  $h \geq 16$  mm, the sample noise and resistance remained almost unvaried. With decreasing distance (increasing ethanol vapor concentration), resistance  $R_0$  decreased, and, at the minimal gap between PD and liquid (1 mm), was almost the same as that for PD submerged in ethanol. It is possible to assume that molecules absorbed on the surface initiate modification of the near-surface band structure, which causes variation in the near-surface layer conductivity [16]. Due to a large thickness of the  $p$ -InAsSbP layer, the effect of possible penetration of molecules towards the bulk  $p$ - $n$ -junction (parallel to axis  $Z$  in Fig. 1,  $a$ ) may be ignored. Thus, the resistance was varying due to emergence and growth of the surface leakage current with decreasing  $h$ .

This assumption was confirmed by the dependence of the diode forward current at fixed voltage  $U_{fb} = 4$  mV on the height above the ethanol surface (triangles in Fig. 3). Since the PD bulk resistance does not change with varying

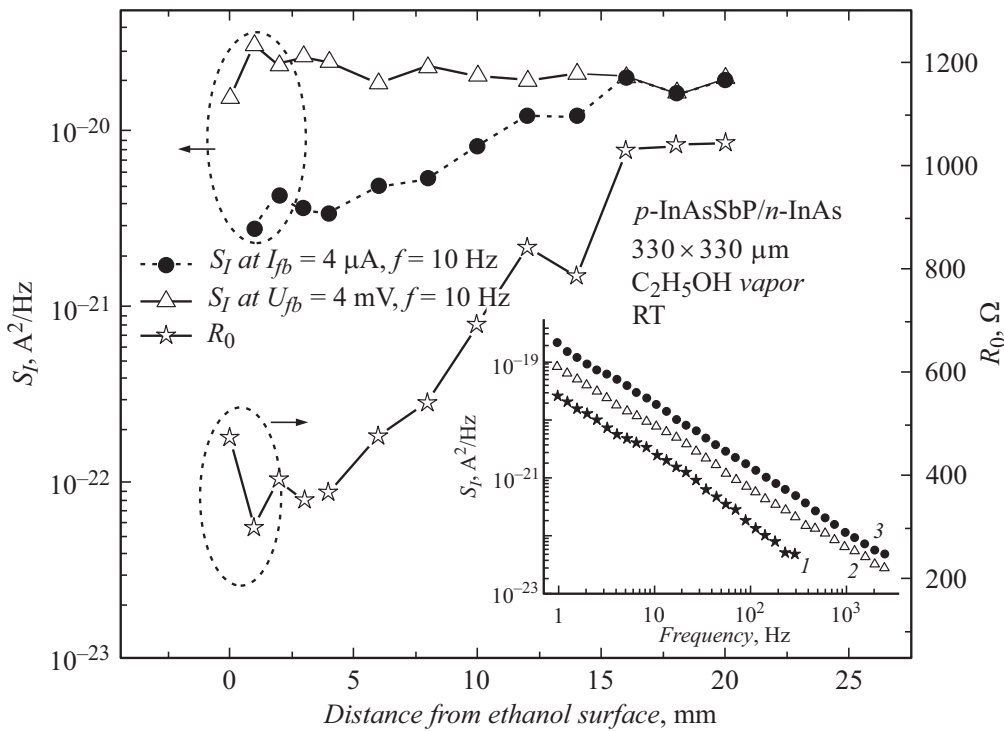


**Figure 3.** Dependences of spectral density of low-frequency current noise  $S_I$  with the reference analysis frequency  $f = 10$  Hz at a constant forward current through the sample  $I_{fb} = 4 \mu A$  (circles) and constant voltage across the sample  $U_{fb} = 4 mV$  (triangles), as well as of zero-bias resistance  $R_0$  (asterisks), on distance  $h$  between PD and ethanol surface. The inset presents frequency dependences of  $S_I$  at forward current  $I_{fb} = 4 \mu A$  for  $h = 1$  (1), 10 (2) and 20 mm (3).

concentration of ethanol vapor, spectral density of the bulk current noise should also remain constant. The fact that the experimentally observed dependence  $S_I$  at constant  $U_{fb}$  is practically independent of  $h$  shows that the noise of the surface leakage current remains low over the entire range of the ethanol vapor concentration, and the observed noise is of the bulk nature.

In the constant-current mode, spectral density of the forward current noise decreased as the sample was approaching the ethanol surface (circles in Fig. 3). This is evidently connected with the fact that, as the ethanol vapor concentration increases, a larger and larger part of current flows over the sample surface, while its bulk part responsible for current fluctuations decreases. This PD property may be utilized to determine the analyte composition by measuring the noise, since the noise may appear to be more sensitive to the analyte than resistance because of the noise spectral density  $S_I$  proportionality to squared  $R_0$ :  $S_I \sim R_0^2$ . Indeed, as Fig. 3 shows, the 3.5-times variation in resistance  $R_0$  is associated with the constant-current-mode variation in the current noise spectral density by an order of magnitude. Notice that frequency dependences of the noise spectral density are in any case defined as  $S_I \sim 1/f$  (inset of Fig. 3).

Despite no models explaining the obtained experimental data are at present available, sequential measurement of noise and resistance allow, apparently, extension of the

sensor functional capabilities by creating a 2D or even 3D model of the „image“ of analyte (in our case, ethanol or its vapor), which is based on a complex of parameters  $R_0$ ,  $S_I(I)$  and  $S_I(U)$ .

To our opinion, the use of an InAs-based PD with unprotected surface as a sensor for ethanol and its vapors has a number of advantages over sensors based on InAs nanowires. This assertion is argued for, first of all, by high reliability of the sample not exposed to the risk of damaging by current bursts, heating, or contacting the liquid flow. Such samples have a failure interval of many years, which is confirmed by their practical employment in a number of analytical devices [14,15]. The distinction of diodes based on InAsSbP/InAs from the nanowire-based sensor is also the sensitivity „inverse“ with respect to that of nanowires, namely, a decrease in resistance in the presence of ethanol vapor (see Fig. 1–3) instead of an increase. Therefore, it is impossible to assert with full confidence that specific reasons for resistance variation are the same in both cases; however, one can assert that the proposed sensor based on  $p$ -InAsSbP/ $n$ -InAs, as well as the sensor considered in [6], will not be selective to ethanol alone. Therefore, it is impossible to assert with full confidence that specific reasons for resistance variation are the same in both cases; however, we can assert that the proposed sensor based on  $p$ -InAsSbP/ $n$ -InAs, as well as the sensor considered in [6], will not be selective to ethanol alone.

In addition, it should not be forgotten that PD preserves its ability to perform its initial („conventional“) functions also in the atmosphere of ethanol vapors; these functions are detection or generation of infrared radiation at the wavelength of  $3.4\ \mu\text{m}$ . This may be used to create the sensor component/information channel which employs conventional optical techniques for measuring hydrocarbon concentration [14,15].

### Acknowledgements

The authors express their gratitude to A.A. Kapralov, S.A. Karandyshev, A.A. Lavrov, M.A. Remennyoy, and G.Yu. Sotnikova, as well as to „IoffeLED“ LLC, for the assistance in performing this study.

### Financial support

A part of work accomplished at University of Montpellier, CNRS, was supported by the grant from CNRS IRP TeraMIR.

### Conflict of interests

The authors declare that they have no conflict of interests.

### References

- [1] V.I. Nikolaev, A.V. Almaev, B.O. Kushnarev, A.I. Pechnikov, S.I. Stepanov, A.V. Chikiryaka, R.B. Timashov, M.P. Scheglov, P.N. Butenko, E.V. Chernikov, *Tech. Phys. Lett.*, **48** (7), 76 (2022). DOI: 10.21883/TPL.2022.07.54046.19211.
- [2] L.Yu. Fedorov, A.V. Ushakov, I.V. Karpov, *Tech. Phys. Lett.*, **48** (7), 58 (2022). DOI: 10.21883/TPL.2022.07.54041.19197.
- [3] G. Scandurra, J. Smulko, L.B. Kish, *Appl. Sci.*, **10** (17), 5818 (2020). DOI: 10.3390/app10175818
- [4] Y.-C. Lee, P.-L. Yang, Ch.I. Chang, W. Fang, *Proceedings*, **2** (13), 772 (2018). DOI: 10.3390/proceedings2130772
- [5] M.V. Lebedev, *Semiconductors*, **54** (7), 699 (2020). DOI: 10.1134/S1063782620070064.
- [6] V. Demontis, M. Rocci, M. Donarelli, R. Maiti, V. Zannier, F. Beltram, L. Sorba, S. Roddaro, F. Rossella, C. Baratto, *Sensors*, **19** (13), 2994 (2019). DOI: 10.3390/s19132994
- [7] M.A. Kinch, *State-of-the-art infrared detector technology* (SPIE, Bellingham—Washington, 2014), p. 280.
- [8] X. Du, B.T. Marozas, G.R. Savich, G.W. Wicks, *J. Appl. Phys.*, **123** (21), 214504 (2018). DOI: 10.1063/1.5027637
- [9] A.V. Pentsov, S.V. Slobodchikov, N.M. Stus', G.M. Filaretova, *Sposob polucheniya fotodiodov*, avtorskoe svidetel'stvo 1840979, zayavka № 3207490/28 (prioritet ot 15.08.1988, opubl. 20.11.2014), byul. № 32. (in Russian)
- [10] N. Dyakonova, S.A. Karandashev, M.E. Levinshtein, B.A. Matveev, M.A. Remennyi, *Semicond. Sci. Technol.*, **33** (6), 065016 (2018). DOI: 10.1088/1361-6641/aac15d
- [11] G.P. Forcade, Ch.E. Valdivia, S. Molesky, S. Lu, A.W. Rodriguez, J.J. Krich, R. St-Gelais, K. Hinzer, *Appl. Phys. Lett.*, **121** (19), 193903 (2022). DOI: 10.1063/5.0116806
- [12] H. Lin, Z. Zhou, H. Xie, Y. Sun, X. Chen, J. Hao, S. Hu, N. Dai, *Phys. Status Solidi A*, **218** (18), 2100281 (2021). DOI: 10.1002/pssa.202100281
- [13] A. Tkachuk, V. Tetyorkin, A. Sukach, in *2021 Int. Semiconductor Conf. (CAS)* (Romania, 2021), p. 279–282. DOI: 10.1109/CAS52836.2021.9604182
- [14] B.A. Matveev, G.Yu. Sotnikova, *Opt. Spectrosc.*, **127** (2), 322 (2019). DOI: 10.1134/S0030400X19080198.
- [15] A.V. Zagnit'ko, I.D. Matsukov, V.V. Pimenov, S.E. Sal'nikov, D.Yu. Fedin, V.I. Alekseev, S.M. Vel'makin, *Tech. Phys.*, **92** (6), 664 (2022). DOI: 10.21883/TP.2022.06.54410.325-21.
- [16] A. Tseng, D. Lynall, I. Savelyev, M. Blumin, S. Wang, H.E. Ruda, *Sensors*, **17** (7), 1640 (2017). DOI: 10.3390/s17071640

Translated by Solonitsyna Anna